



Transcriptome analysis reveals involvement of thiopurine S-methyltransferase in oxidation-reduction processes

Alenka Šmid^{a,*}, Miha Štajdohar^b, Miha Milek^{a,c}, Dunja Urbančič^a, Nataša Karas Kuželički^a, Riin Tamm^{d,e}, Andres Metspalu^d, Irena Mlinarič-Raščan^{a,*}

^a Department of Clinical Biochemistry, Faculty of Pharmacy, University of Ljubljana, Slovenia

^b Genialis Inc., Boston, MA, USA

^c Core Unit Bioinformatics, Berlin Institute of Health at Charite, Germany

^d Estonian Genome Center, Institute of Genomics and Institute of Molecular and Cell Biology, University of Tartu, Estonia

^e Youth and Talent Policy Department, Estonian Ministry of Education and Research, Estonia

ARTICLE INFO

Keywords:

Thiopurine S-methyltransferase
Transcriptome
Data fusion by matrix factorization
Oxidation–reduction processes
RNA microarray profiling

ABSTRACT

Thiopurine S-methyltransferase (TPMT) is an important enzyme involved in the deactivation of thiopurines and represents a major determinant of thiopurine-related toxicities. Despite its well-known importance in thiopurine metabolism, the understanding of its endogenous role is lacking. In the present study, we aimed to gain insight into the molecular processes involving TPMT by applying a data fusion approach to analyze whole-genome expression data. The RNA profiling was done on whole blood samples from 1017 adult male and female donors to the Estonian biobank using Illumina HTv3 arrays. Our results suggest that TPMT is closely related to genes involved in oxidoreductive processes. The *in vitro* experiments on different cell models confirmed that TPMT influences redox capacity of the cell by altering S-adenosylmethionine (SAM) consumption and consequently glutathione (GSH) synthesis. Furthermore, by comparing gene networks of subgroups of individuals, we identified genes, which could have a role in regulating TPMT activity. The biological relevance of identified genes and pathways will have to be further evaluated in molecular studies.

1. Introduction

Thiopurine drugs, such as azathioprine and 6-mercaptopurine (6-MP), are cytotoxic and immunosuppressive drugs used in the treatment of acute lymphoblastic leukemia (ALL), inflammatory bowel disease, autoimmune disorders and to prevent rejection after organ transplantation (Lennard, 1992). The efficacy and safety of thiopurine drugs display large interindividual variability which can be explained, to a large extent, by genetic polymorphisms of thiopurine S-methyltransferase (TPMT), a cytosolic enzyme which S-methylates and deactivates thiopurines. The distribution of TPMT activity in Caucasian populations is trimodal approximately 89% of the population shows normal to high, 11% intermediate and 0.3% low or undetectable TPMT activity (Weinshilboum and Sladek, 1980; Yates et al., 1997). TPMT-deficient patients tend to be better responders to 6-MP therapy than patients with normal or high TPMT activity due to higher concentrations of active thioguanine nucleotide (TGN) but are at a greater risk of developing toxic effects such as bone marrow suppression,

infections and stomatitis (Evans, 2004). On the other hand, ultra-high enzyme activity can lead to superior 6-MP tolerability but also to an increased risk of relapse and hepatic toxicity, which has been related to methylated metabolites of thiopurines (Evans, 2004). To date 46 variant alleles in the TPMT gene have been identified (Appell et al., 2013), of which three (*TPMT*2*, *TPMT*3A* and *TPMT*3C*) cause up to 95% of all low TPMT enzyme activities and are thus the most clinically important (Appell et al., 2013; Relling et al., 2011; Zimdahl Kahlin et al., 2021). In general individuals with two non-functional alleles have very low or undetectable TPMT activity, those carrying only one variant allele have intermediate and individuals with no variant alleles normal to high activity. However, the concordance between genotype and phenotype is not complete, especially in heterozygous individuals, where the concordance can be as low as 50% (Lennard et al., 2013; Schaeffeler et al., 2004; Zimdahl Kahlin et al., 2021). Identification of new biomarkers influencing TPMT activity could therefore improve individualization of thiopurine therapy.

Besides the above mentioned variants in the coding region of *TPMT*,

* Corresponding authors.

E-mail addresses: alenka.smid@ffa.uni-lj.si (A. Šmid), irena.mlinaric@ffa.uni-lj.si (I. Mlinarič-Raščan).

<https://doi.org/10.1016/j.ejps.2023.106616>

Received 18 July 2023; Received in revised form 18 October 2023; Accepted 18 October 2023

Available online 19 October 2023

0928-0987/© 2023 The Authors. Published by Elsevier B.V. This is an open access article under the CC BY-NC-ND license (<http://creativecommons.org/licenses/by-nc-nd/4.0/>).

the enzyme activity can be influenced by the variable number of tandem repeat (VNTR) located in *TPMT* promoter region which influences gene expression levels (Kotur et al., 2015; Spire-Vayron de la Moureyre et al., 1998; Urbančić et al., 2018) as well as by other genetic and non-genetic factors. Of genetic factors, the polymorphism rs2413739 in *PACSN2*, was found to modulate *TPMT* activity and influence mercaptopurine-induced toxicity in ALL patients (Stocco et al., 2012; Franca et al., 2020; Šmid et al., 2016). *In vitro* studies show that *PACSN2* inhibits autophagy, which might influence thiopurine sensitivity, whereas the modulation of *TPMT* activity probably happens via mechanisms distinct from its modulation of autophagy (Zudeh et al., 2023). Of non-genetic factors, *S*-adenosylmethionine (SAM) was shown to significantly influence *TPMT* activity in our previous *in vitro* studies using cell models (Milek et al., 2012, 2009, 2006) as well as *in vivo* study on human subjects (Karas-Kuzelićki et al., 2014). Among other non-genetic factors gender (Gisbert et al., 2007), age (McLeod et al., 1995; Serpe et al., 2009), and concomitant drugs, such as methotrexate (Wennerstrand et al., 2013), were reported to influence *TPMT* activity in some studies.

While *TPMT* function on metabolism of thiopurines is well characterized and represents an important determinant of toxicity caused by these drugs, its biological role remains obscure. Recently, recombinant *TPMT* has been shown to catalyze methylation of selenocysteine *in vitro* which indicates *TPMT* might have a role in detoxifying compounds with selenol groups (Urbančić et al., 2019), and was found to catalyze production of trimethylselenium ion, enabling urinary excretion of selenium (Fukumoto et al., 2020). Moreover, *TPMT* was identified as an enzyme involved in molybdenum cofactor catabolism (Pristup et al., 2022). Further studies on the endogenous role of *TPMT* in intracellular metabolism and mechanisms of its regulation are needed and would provide an important source of knowledge, based on which new candidate markers could be selected for further validation studies.

The aim of this study was to get a new insight into endogenous function of *TPMT* using blood-based gene expression profiles of healthy volunteers. For this purpose we applied a data fusion approach with penalized matrix tri-factorization (Zitnik and Zupan, 2014). This approach enables integration of diverse data sources and is applicable to problems such as prediction of regulatory, metabolic and other functional classes, and prediction of protein interactions (Zitnik and Zupan, 2014). To identify genetic mechanisms, which besides the *TPMT* genotype, may underlie differences in *TPMT* activity, we additionally constructed and analyzed predictive models in subgroups of individuals divided on the basis of *TPMT* genotype to phenotype concordance.

2. Materials and methods

2.1. Subjects

One thousand and seventeen volunteer donors to the Estonian Biobank (Estonian Genome Centre, n.d.) were included in this study, which was approved by the Research Ethics Committee (University of Tartu, Estonia). Informed consent was obtained from all donors. Venous blood (50 mL) was drawn into a K₃-EDTA tube and processed at less than 12 h after collection. RBCs were used for hemolysate preparation in which *TPMT* activity was measured. One aliquot was used for DNA extraction and another aliquot which was drawn into Tempus Blood RNA Tube was used for RNA extraction. The demographic data of the donors (including age, and gender) were extracted from the Biobank database. The cohort consisted of 511 (50.2%) males and 504 (49.8%) females, with a median age of 34 years (IQR 25–47). There was no statistically significant difference in age between males (median = 33, IQR = 25–45) and females (median = 35, IQR = 24–49). In total, 961 subjects had the wild-type *TPMT* genotype (*TPMT**1/*1), while 56 were heterozygous (*TPMT**1/*3). Of the 56 heterozygous individuals, 50 were *TPMT**1/*3A and six were *TPMT**1/*3C. No variant homozygotes (*TPMT**3/*3) were found in the study cohort. No *TPMT**2 alleles were

present.

2.2. Hemolysate preparation

Hemolysates were prepared in accordance with the previously described procedure (Milek et al., 2006; Keizer-Garritsen et al., 2003). An aliquot of 0.1 mL was used for the hemoglobin (Hb) measurement (Coulter AcT Diff analyzer, Beckman Coulter, Brea, CA).

2.3. *TPMT* activity measurement and cut-off determination

TPMT activity was measured in RBCs hemolysates using the HPLC method as previously described (Milek et al., 2012, 2009, 2006; Wang et al., 2001). Briefly, for *TPMT* activity measurements the RBC hemolysates were incubated with SAM (90 μmol/L), dithiothreitol (450 μmol/L), allopurinol (36 μmol/L) and 6-MP (4,3 mmol/L) in potassium phosphate buffer. The reaction was stopped by addition of HClO₄. The supernatant was neutralized with K₂HPO₄ before being used for HPLC analysis. Samples were eluted with a mobile phase containing 75% of 50 mM potassium phosphate buffer (pH=7,5) and 25% methanol at flow rate of 1,5 mL/min and 6-methylmercaptopurine was detected and quantified at wavelength 290 nm. Agilent Technologies 1100 HPLC system and Chemstation for LC 3D Systems software were used. The recovery of all analyzed metabolites was evaluated by spiking known amounts of standards into biological samples and was found to be higher than 95% for all analyses. An average value of two independent measurements was reported for all analyses.

The cut-off value for *TPMT* activity (26.1 nmol/g Hb/h) was obtained by receiver-operating characteristic (ROC) analysis (GraphPad Prism 5) (Karas-Kuzelićki et al., 2014). The *TPMT* activity values above this cut-off belong to the normal range expected in individuals with wild-type *TPMT* genotype, while those below it are expected in *TPMT*-heterozygous individuals. In this paper, we used the term normal *TPMT* activity for values above the determined cut-off value of 26.1 nmol/g Hb/h and low *TPMT* activity was used for values below the mentioned cut-off value.

2.4. DNA and RNA extraction

DNA was extracted using the conventional salting out procedure (Miller et al., 1988). The genotyping of the *TPMT* activity-deficient *TPMT**3B (460G>A, rs1800460), *3C (719A>G, rs1142345) and *2 (283G>C, rs1800462) alleles was carried out by TaqMan Genotyping Assays (Applied Biosystems, Foster City, CA), as described previously (Karas Kuzelićki et al., 2009). Alleles *3B and *3C inherited together in *cis* represent the *3A alleles (460G>A and 719A>G).

RNA was extracted using Tempus Spin RNA Isolation Kit (Life Technologies, NY, USA) and quantified by NanoDrop 1000 Spectrophotometer (Thermo Fisher Scientific, DE, USA). RNA integrity was assessed by Agilent 2100 Bioanalyzer (Agilent Technologies, CA, USA). Samples with RIN<7.0 were excluded.

2.5. Amplification, labeling and BeadChip hybridization

Ambion TotalPrep RNA Amplification Kit (Life Technologies, NY, US) was used to transcribe 200 ng RNA according to the manufacturer's recommendation which was then hybridized to the Illumina HT12v3 arrays (Illumina Inc, San Diego, US) according manufactures protocols.

2.6. Data pre-processing

The BeadChips were scanned with the Illumina HiScan system. After background subtraction, raw intensity data was exported using the Illumina GenomeStudio software. Further data processing was conducted by means of R language and appropriate Bioconductor modules. Data was log₂-transformed and normalized using robust spline

normalization (rsn) method, both steps were performed using lumi pipeline (Du et al., 2008). Data were subsequently normalized to values between 0 and 1 and missing values were filled-in with 0.

2.7. Data collections and data fusion

We modelled gene associations with 6 data sets that describe the involvement of TPMT in intracellular processes from various perspectives. We used a data fusion approach with penalized matrix tri-factorization, called data fusion by matrix factorization (Zitnik and Zupan, 2014) that simultaneously factorizes many heterogeneous data matrices to reveal hidden associations. The approach can directly consider any data that can be expressed in a matrix, including those from feature-based representations, ontologies, associations and networks.

The model considered 3 types of objects: genes, GO terms, and subjects (nodes in Fig. 1). Six data sets (matrices) were built on these objects, each relating a pair of object types (arcs in Fig. 1). The $R_{1,2}$ relation matrix represents the relation between subjects and gene expression levels. Gene IDs (names and nuIDs) were mapped to Genebank IDs. The $R_{2,3}$ matrix represents relation between genes and GO terms. The $R_{1,3}$ relation matrix represents the relation between subject and GO term and was created indirectly via relation matrices $R_{1,2}$ and $R_{2,3}$. Genes from $R_{1,2}$ (nuID) which are contained also in the Gene Ontology database (uniprot) were mapped to common ID (Genebank ID).

Protein-protein interactions were included as constraints between corresponding genes. Proteins from the STRING database (<http://string-db.org>) annotated by Genbank ID were used to build the constraint matrix Θ_2 . Degrees of interactions were normalized to values between 0 and -1. In case of no known interaction, the value was 0. Hierarchical structure of GO (Θ_3) was included by reasoning over *has_part*, *part_of* and *is_a* relations in the GO graph. A constraint between a pair of GO terms was set to -0.2^{hops} , where hops was the length of the shortest path between the two GO terms.

The data fusion by matrix factorization was applied to predict the genetic factors involved in gene regulatory network of TPMT. The predictive model learns from relations (R) between objects of different types considering the constraints (Θ) to the objects of the same type. The

final model is schematically presented in Fig. 1.

Data fusion was performed in three steps. First, data were encoded in constraint and relations matrices and organized in a block-based matrix representation. In the second step, relation matrices $R_{i,j}$ were simultaneously tri-factorized given constraints in Θ_i . Finally, matrix factors were used to reconstruct the relation matrices $R_{1,2}$ and $R_{2,3}$ that included the fused knowledge from all data sources.

Five predictive models were built: (0) including all subjects ($N = 1017$), (I) including subjects with wild-type TPMT genotype and normal TPMT activity ($N = 818$), (II) including subjects with heterozygous TPMT genotype and low TPMT activity ($N = 46$), (III) including subjects with wild-type TPMT genotype and low TPMT activity ($N = 143$), and (IV) including subjects with heterozygous TPMT genotype and normal TPMT activity ($N = 10$).

2.8. Cell culture

For routine culturing HepG2 (ATCC, LGC Promochem, Wesel, Germany) and COS-7 cells (DSMZ, Braunschweig, Germany) were grown in Dulbecco's modified Eagle's medium, supplemented with 10% FBS (Gibco, Carlsbad, CA, USA), 2 mM L-glutamine and 100 U/ml penicillin/streptomycin. Cultures were incubated in a sterile environment at 37 °C with a humidified atmosphere of 5% CO₂.

HepG2 cells stably expressing the N-terminal EGFP-TPMT fusion protein (TPMT+) were prepared and characterized as described previously (Egle et al., 2008) and were cultured in the same media as untransfected (UT) HepG2 cells as described above.

COS-7 cells were transfected with various TPMT cDNAs (TPMT*1, *2, *3A, *3C) as described previously (Milek et al., 2012).

2.9. Cell proliferation and viability

Cells were seeded into 96-well plates (8×10^3 /well) and incubated overnight. On the next day, cells were incubated for various time periods with the substances indicated in Figure legends. In some experiments, cells were pre-incubated with N-acetylcysteine (NAC) for 2 h, followed by incubation with 25 μ M N-ethylmaleimide (NEM) for 4 h. Metabolic activity, as an indication of cell proliferation, was determined by the

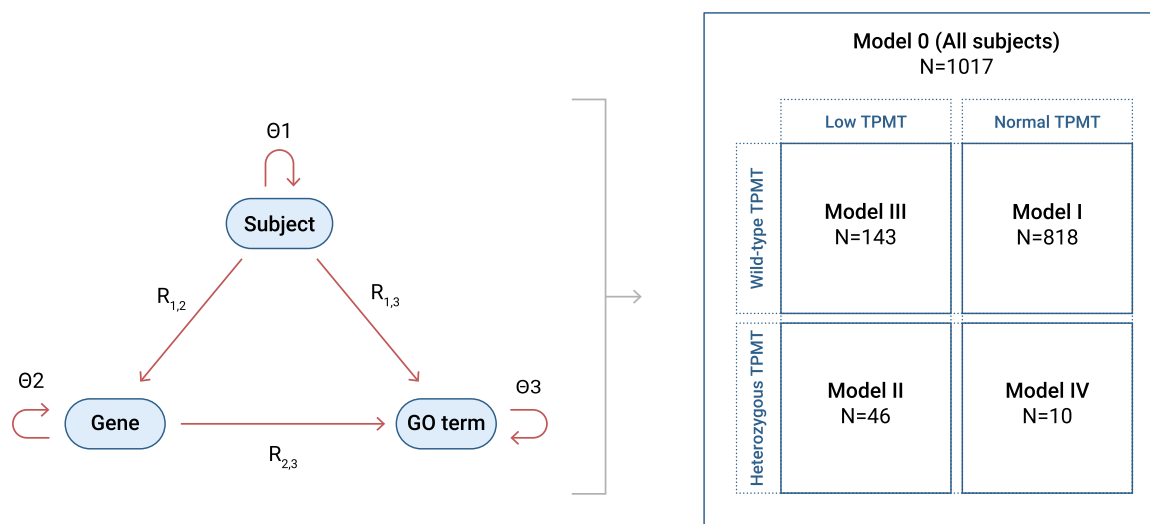


Fig. 1. The fusion configuration for TPMT gene network prediction.

Nodes represent 3 object types. Arcs denote data sets that relate objects of different types (relation matrices, $R_{i,j}$) or objects of the same type (constraints, Θ_i) for a total of 6 matrices (data sets). Fused data sets include gene annotations ($R_{2,3}$); expression profiles ($R_{1,2}$); subject-GO relation matrix ($R_{1,3}$). Constraint matrices encode groups of subjects according to genotype-phenotype correlation (Θ_1), protein-protein interactions (Θ_2), and semantic structure of the Gene Ontology graph (Θ_3). Five models were built: (0) including all subjects ($N = 1017$), (I) including subjects with wild-type TPMT genotype and normal TPMT activity ($N = 818$), (II) including subjects with heterozygous TPMT genotype and low TPMT activity ($N = 46$), (III) including subjects with wild-type TPMT genotype and low TPMT activity ($N = 143$), and (IV) including subjects with heterozygous TPMT genotype and normal TPMT activity ($N = 10$).

CellTiter Aqueous One Proliferation Assay, while ATP content, as an indication of cell viability, was determined by the CellTiter Glo Luminescent Cell Viability Assay (both from Promega, Madison, WI, USA) on an automated plate reader (Tecan Safire2, Zürich, Switzerland) as described (Milek et al., 2009). In some experiments, viability was determined by Trypan blue exclusion.

2.10. Oil red O staining and microscopy

To detect cellular lipid accumulation, HepG2 cells were stained by the Oil Red O method as described (Lin et al., 2007). Briefly, following treatment with H₂O₂, cells were washed three times with PBS and fixed with 10% formalin for 60 min. After fixation, cells were washed and stained with Oil Red O solution for 60 min at room temperature and then washed with water. Transmission images were acquired on a CKX41 microscope using C-7070 camera (Olympus).

3. Results and discussion

3.1. Examination of the constructed gene association network suggests that *TPMT* is closely related to oxidation–reduction processes

The first model of *TPMT* gene association network was built for all subjects independently of their *TPMT* genotype-phenotype status (Model 0). The network includes genes in the nodes that are connected based on the distance function, defined as the average Euclidean distance between genes in the inferred relation matrices $R_{1,2}$ and $R_{2,3}$. The section of the gene association network in proximity to *TPMT* is depicted in Fig. 2.

Genes most similar to *TPMT* based on the computed distances (highlighted by the red square in Fig. 2)— including but not limited to *PAICS*, *PPAT*, *GMPS* and *MTHFR*—were analyzed with DAVID's functional annotation clustering tool (Huang et al., 2009a, 2009b). Several enriched annotation clusters were detected, with the most notable ones associated with oxidoreductive processes and nucleotide and pigment

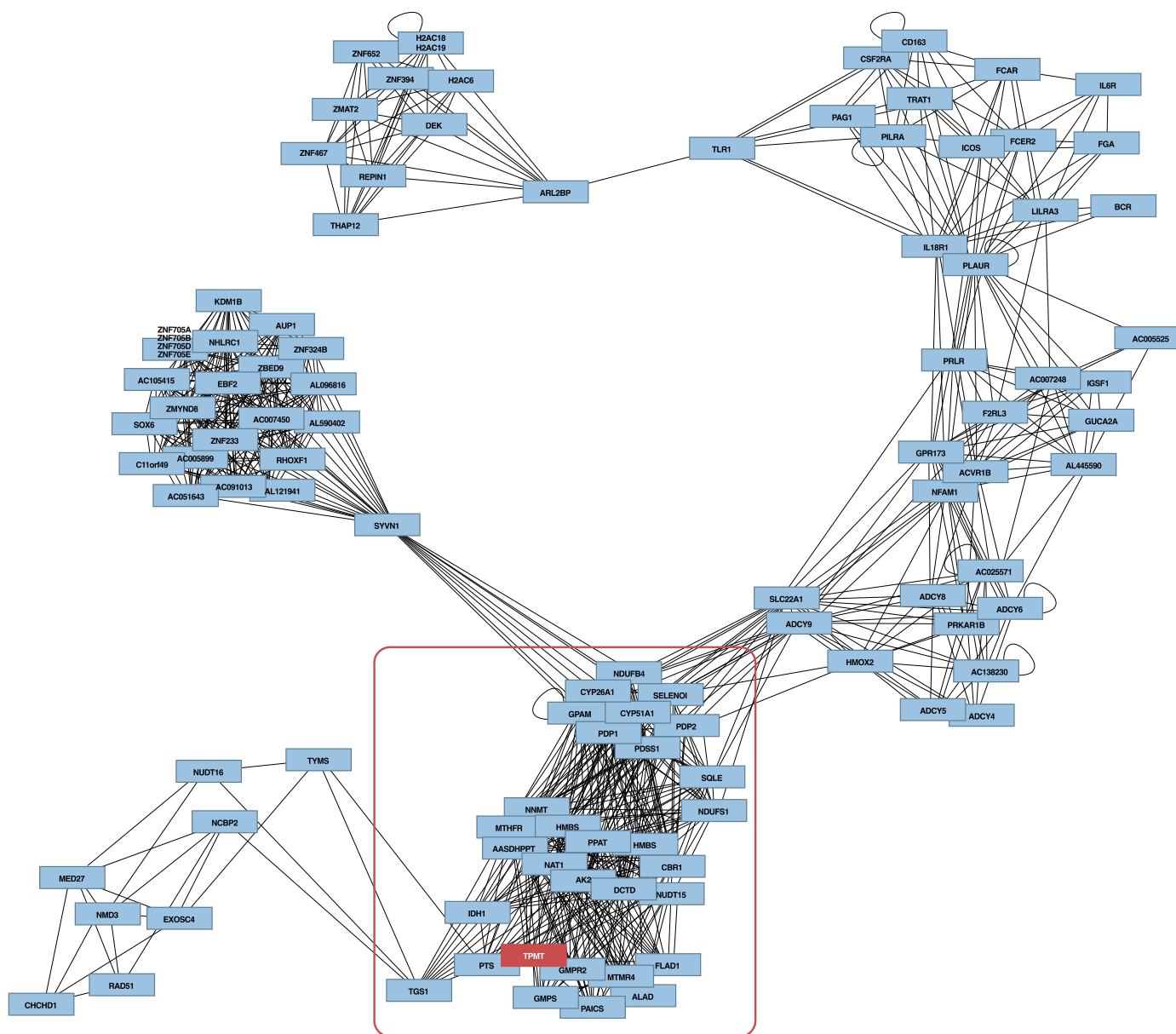


Fig. 2. A part of a gene network showing genes clustered around *TPMT* constructed from the model for all subjects.

Nodes represent genes and arches relations between genes. *TPMT* is represented by a red node. The list of genes in the red square, which were analyzed by DAVID functional annotation tool, is available in Supplementary Table S1.

biosynthetic processes. The top 5 clusters are presented in Table 1.

The most enriched cluster of functional annotation within the TPMT network was discovered to be linked to oxidoreductive processes and includes the following genes: NADH-ubiquinone oxidoreductase B15 Subunit (*NDUFB4*), carbonyl reductase 1 (*CBR1*), 5,10-methylenetetrahydrofolate reductase (*MTHFR*), guanosine monophosphate reductase 2 (*GMPR2*), cytochrome P450, family 51, subfamily A, polypeptide 1 (*CYP51A1*), squalene epoxidase (*SQLE*), soluble isocitrate dehydrogenase 1 (*IDH1*), cytochrome P450, family 26, subfamily A, polypeptide 1 (*CYP26A1*), and NADH dehydrogenase (ubiquinone) Fe-S protein 1 (*NDUFS1*). Two of the genes (*NDUFS1* and *NDUFB4*) form the part of the

mitochondrial membrane respiratory chain NADH dehydrogenase (Complex I), which is essential for the production of mitochondrial ATP (Hoefs et al., 2010). *IDH1* has a significant role in cytoplasmic NADPH production (Geisbrecht and Gould, 1999), whereas other genes in the cluster utilize NADPH as the cofactor in their enzymatic reactions. NADPH is also a critical molecule for the maintenance of antioxidant cell capacity through the regeneration of reduced pools of glutathione (Santos et al., 2011). TPMT on the other hand is a methyltransferase utilizing SAM as a methyl donor and directly influences cell's methylation capacity as measured by SAM/SAH ratio. Metabolically, cell methylation and redox capacity (measured by ratio of reduced and

Table 1
Functional annotation clustering of TPMT gene network using DAVID tools (top 5 clusters).

Cluster 1	Enrichment Score: 3.8923084803846044			
Category	Term	#	P	B
SP_PIR_KEYWORDS	oxidoreductase	9	1.26E-06	1.30E-04
GOTERM_BP_FAT	GO:0,055,114~oxidation-reduction	9	8.90E-06	5.11E-04
SP_PIR_KEYWORDS	nadp	5	8.44E-05	0.001738
GOTERM_CC_FAT	GO:0,000,267~cell fraction	4	0.284677	0.663387
<i>NDUFB4, CBR1, MTHFR, GMPR2, CYP51A1, SQLE, IDH1, CYP26A1, NDUFS1</i>				
Cluster 2	Enrichment Score: 3.53562638605005			
Category	Term	#	P	B
SP_PIR_KEYWORDS	magnesium	8	3.25E-06	1.12E-04
GOTERM_MF_FAT	GO:0,000,287~magnesium ion binding	7	3.38E-04	0.037792
SP_PIR_KEYWORDS	manganese	4	0.00152	0.019399
GOTERM_MF_FAT	GO:0,030,145~manganese ion binding	4	0.004314	0.218397
<i>PDP1, PDP2, AASDHPPT, NUDT15, IDH1, EPT1, PDSS1, PPAT</i>				
Cluster 3	Enrichment Score: 3.1958218430584244			
Category	Term	#	P	B
GOTERM_BP_FAT	GO:0,046,148~pigment biosynthetic process	5	6.01E-07	1.38E-04
GOTERM_BP_FAT	GO:0,042,440~pigment metabolic process	5	1.08E-06	8.29E-05
GOTERM_BP_FAT	GO:0,009,113~purine base biosynthetic process	3	1.08E-04	0.004123
SP_PIR_KEYWORDS	purine biosynthesis	3	1.44E-04	0.002461
GOTERM_BP_FAT	GO:0,006,144~purine base metabolic process	3	2.71E-04	0.007761
GOTERM_BP_FAT	GO:0,046,112~nucleobase biosynthetic process	3	2.71E-04	0.007761
GOTERM_BP_FAT	GO:0,009,165~nucleotide biosynthetic process	5	2.96E-04	0.007548
GOTERM_BP_FAT	GO:0,034,654~nucleobase, nucleoside, nucleotide and nucleic acid biosynthetic process	5	3.41E-04	0.007818
GOTERM_BP_FAT	GO:0,034,404~nucleobase, nucleoside and nucleotide biosynthetic process	5	3.41E-04	0.007818
GOTERM_BP_FAT	GO:0,009,127~purine nucleoside monophosphate biosynthetic process	3	4.54E-04	0.009441
GOTERM_BP_FAT	GO:0,009,168~purine ribonucleoside monophosphate biosynthetic process	3	4.54E-04	0.009441
GOTERM_BP_FAT	GO:0,009,126~purine nucleoside monophosphate metabolic process	3	5.62E-04	0.010718
GOTERM_BP_FAT	GO:0,009,167~purine ribonucleoside monophosphate metabolic process	3	5.62E-04	0.010718
GOTERM_BP_FAT	GO:0,009,112~nucleobase metabolic process	3	7.46E-04	0.012185
GOTERM_BP_FAT	GO:0,009,156~ribonucleoside monophosphate biosynthetic process	3	7.46E-04	0.012185
GOTERM_BP_FAT	GO:0,009,161~ribonucleoside monophosphate metabolic process	3	8.83E-04	0.013449
GOTERM_BP_FAT	GO:0,009,150~purine ribonucleotide metabolic process	4	0.001797	0.025522
GOTERM_BP_FAT	GO:0,009,259~ribonucleotide metabolic process	4	0.002152	0.028729
GOTERM_BP_FAT	GO:0,009,124~nucleoside monophosphate biosynthetic process	3	0.003508	0.041648
GOTERM_BP_FAT	GO:0,006,163~purine nucleotide metabolic process	4	0.004185	0.044891
KEGG_PATHWAY	hsa00230:Purine metabolism	5	0.004465	0.105841
GOTERM_BP_FAT	GO:0,009,123~nucleoside monophosphate metabolic process	3	0.006037	0.061348
GOTERM_BP_FAT	GO:0,009,152~purine ribonucleotide biosynthetic process	3	0.01808	0.149047
GOTERM_BP_FAT	GO:0,009,260~ribonucleotide biosynthetic process	3	0.020165	0.159312
GOTERM_BP_FAT	GO:0,006,164~purine nucleotide biosynthetic process	3	0.028033	0.195869
<i>ALAD, HMBS, PAICS, GMPS, PPAT</i>				
Cluster 4	Enrichment Score: 2.8812613290200364			
Category	Term	#	P	B
GOTERM_BP_FAT	GO:0,051,186~cofactor metabolic process	6	2.01E-05	9.25E-04
GOTERM_BP_FAT	GO:0,006,733~oxidoreduction coenzyme metabolic process	3	0.003789	0.042718
GOTERM_BP_FAT	GO:0,006,732~coenzyme metabolic process	3	0.029806	0.201088
<i>CBR1, ALAD, HMBS, IDH1, FLAD1, PDSS1</i>				
Cluster 5	Enrichment Score: 2.3439223059144876			
Category	Term	#	P	B
GOTERM_BP_FAT	GO:0,051,186~cofactor metabolic process	6	2.01E-05	9.25E-04
GOTERM_BP_FAT	GO:0,018,130~heterocycle biosynthetic process	4	1.49E-04	0.004898
GOTERM_BP_FAT	GO:0,051,188~cofactor biosynthetic process	4	6.48E-04	0.01141
SP_PIR_KEYWORDS	alternative splicing	7	0.989245	1
UP_SEQ_FEATURE	splice variant	7	0.989518	1
<i>CBR1, ALAD, HMBS, IDH1, FLAD1, PDSS1</i>				

Abbreviations: P = p-value, B = Benjamini corrected p-value.

oxidized form of glutathione, GSH/GSSG ratio) are linked through one-carbon metabolism involving folate and methionine cycle and the transsulfuration pathway. When SAM is used a methyl donor *S*-adenosylhomocysteine (SAH) is produced and subsequently hydrolyzed by the SAH hydrolase to homocysteine and adenosine. Homocysteine can then be either remethylated to methionine from which SAM can be synthesized or irreversibly removed from the methionine cycle by cystathionine beta synthase (CBS) which initiates the transsulfuration pathway for the synthesis of cysteine and glutathione, body's primary antioxidant (James et al., 2006). Although increased oxidative stress and DNA hypomethylation have often been detected together (Franco et al., 2008), the mechanism of this co-occurrence has not been fully elucidated yet. One of the possible explanations is that GSH depletion under conditions of oxidative stress may lead to decreased global DNA methylation through the depletion of SAM (Hitchler and Domann, 2007). Under oxidizing conditions, cystathionine- β -synthase (CBS) activity increases to direct homocysteine (Hcy) flux through the transsulfuration pathway for the generation of GSH (Mosharov et al., 2000). Consequently, less Hcy is directed toward the regeneration of methionine, which may result in decreased SAM levels.

3.2. In vitro studies show that TPMT influences antioxidant capacity of the cell

3.2.1. Overexpressed TPMT results in increased toxicity of oxidative stress inducers in HepG2 cells

To determine the influence of differential expression of TPMT on cell proliferation and viability upon induction of oxidative stress we have used HepG2 cells stably transfected with a pEGFP-TPMT construct (TPMT+) (Egle et al., 2008) as well as untransfected HepG2 cells (UT). When cells were incubated with identical concentrations of oxidative stress inducers (e.g. 1 mM H₂O₂, 20 μ M NEM) higher toxicity as determined by cell proliferation and viability was observed in the TPMT+ cells relative to UT cells (Fig. 3A, B). No differential response between TPMT+ and UT cells was observed when apoptosis inducers (TPCK, DMSO, Fig. 3C) were tested. Furthermore, after treatment of cells with the same amount of H₂O₂ and staining with Oil Red O, increased number of lipid vesicles and necrotic morphology were observed in TPMT+ cells compared to UT cells (Fig. 4).

To determine whether TPMT influences cell survival by modulating synthesis of the major cellular antioxidant, GSH, cells were pre-incubated with NAC, a precursor of cysteine and GSH. Compared to UT cells, significantly higher NAC concentrations were required in TPMT+ cells to prevent cell death induced by NEM, a GSH-depleting agent (Fig. 5A). This led us to hypothesize that high cellular TPMT may decrease the SAM flux through the Met-cycle and consequently limit GSH synthesis. To confirm that TPMT modulates cell redox capacity, total intracellular GSH concentrations were measured in untreated, H₂O₂- and NEM-treated untransfected or TPMT+ cells. Significantly lower GSH levels were observed in TPMT+ cells than in UT cells in untreated, as well as in H₂O₂- and NEM-treated cells (Fig. 5B). These results show that, on induction of oxidative stress, cell death depends on TPMT status. Higher TPMT activity correlates with more rapid GSH depletion, which impacts redox capacity and antioxidant response of hepatocellular carcinoma cells.

3.2.2. Intracellular SAM and GSH levels correlate with TPMT activity

To elucidate the effect of TPMT variant proteins on redox metabolism, we transiently co-transfected COS-7 cells with plasmids containing cDNAs coding for four TPMT allozymes resulting from most common TPMT genetic polymorphisms (TPMT*1, *2, *3A, *3C). Significantly lower SAM and GSH levels were observed 24 and 48 h post-transfection in TPMT*1-transfected cells compared to mock control (pcDNA) cells (Fig. 6B,C). In TPMT*3C-transfected cells, significantly lower SAM and GSH levels were observed only at 24-hour time point, but not at 48 h after transfection. SAM and GSH levels were not

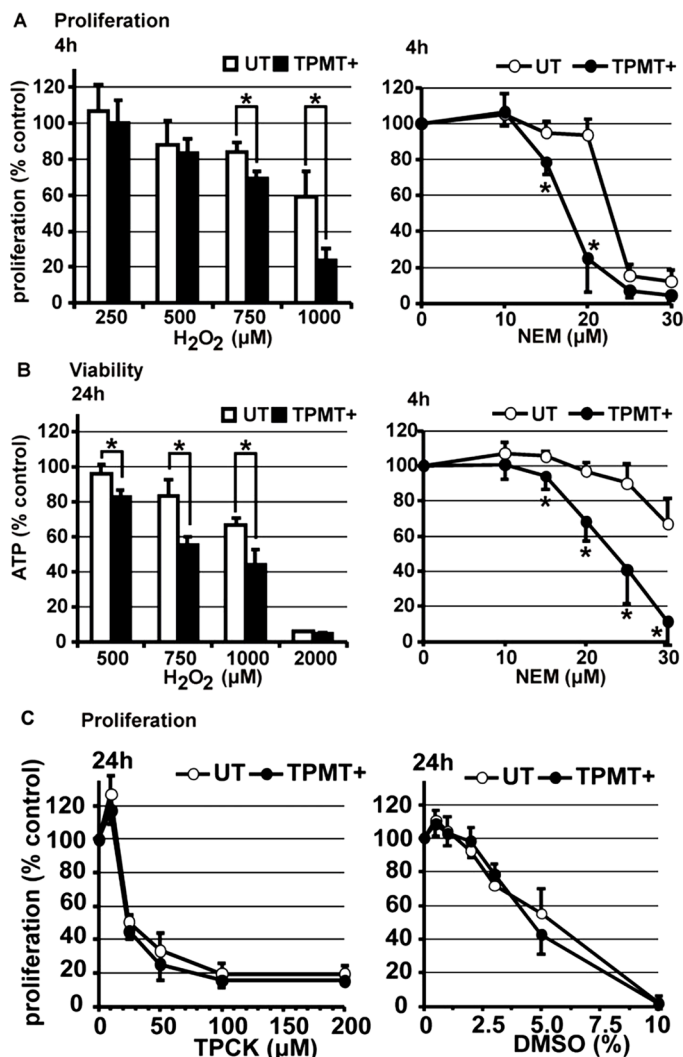


Fig. 3. Overexpression of TPMT results in higher sensitivity to oxidative stress inducers, but not apoptosis inducers.

Cell proliferation (A) and viability (B) were determined after untransfected (UT) and TPMT+ HepG2 cells were incubated in the presence of increasing concentrations of oxidative stress inducers (H₂O₂ and NEM) for the indicated time periods. Cell proliferation (C) was determined also after UT or TPMT+ HepG2 cells were incubated in the presence of increasing concentrations of apoptosis inducers (TPCK or DMSO) for the indicated time periods.

significantly altered in TPMT*2 and TPMT*3A-transfected cells. It has been shown, that among variant alloenzymes, TPMT*2 and *3A are degraded most rapidly via the proteasome pathway, followed by TPMT*3C and the wild-type protein (TPMT*1) (Tai et al., 1997). Our results thus indicate that high intracellular TPMT activity and protein levels (TPMT*1 and *3C) are associated with lower SAM and GSH concentrations while rapid TPMT degradation (TPMT*2 and *3A) does not change the cell redox and methylation capacity. This suggests that consumption of SAM is significantly faster in cells with high TPMT activity (TPMT*1) and that the metabolic flux of SAM towards GSH synthesis is decreased, resulting in lower antioxidant capacity of the cell. The proposed mechanism of TPMT modulation of oxidative stress by influencing GSH levels is schematically presented in Supplementary Fig. S1.

3.3. Identification of new candidate genes with the potential influence on TPMT activity

To find out the differences in TPMT gene associated network between

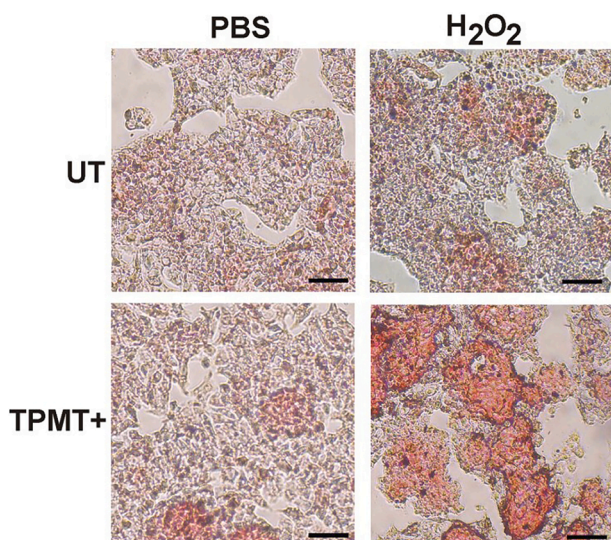
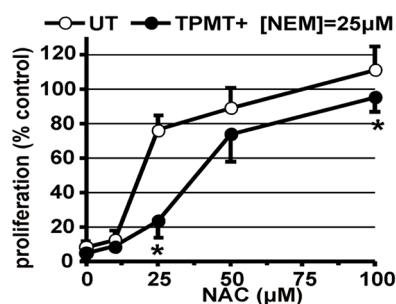


Fig. 4. Steatosis in H_2O_2 -induced cell death. After incubation in FBS-free Met⁺ medium for 48 h, UT and TPMT⁺ cells were incubated with PBS or H_2O_2 (5 mM) for 4 h, followed by fixation and lipid staining with Oil red O. Representative transmission images are shown. Magnification, 20 ×; scale bar, 50 μm.

A Proliferation



B

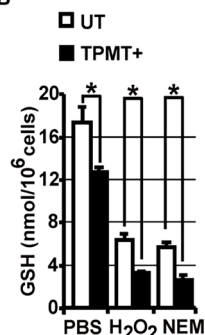


Fig. 5. TPMT modulates cell redox capacity.

(A) UT or TPMT⁺ cells were pre-incubated with increasing NAC concentrations (2 h), followed by incubation with fixed concentration of NEM (25 μM, 4 h), and cell proliferation was determined. (B) After incubation in FBS-free Met⁺ medium for 48 h, UT and TPMT⁺ cells were incubated with H_2O_2 (5 mM, 1.5 h) or NEM (100 μM, 1 h) and total intracellular GSH levels were determined spectrophotometrically.

different TPMT genotype-phenotype groups, we constructed four distinct predictive models and conducted a comparative analysis. The models were built for each of the genotype-phenotype groups, which were defined as follows. Two groups were defined as TPMT genotype-phenotype concordant: wild-type individuals with normal activity (Model I) and heterozygous individuals with low activity (Model II). Two groups of individuals were defined as TPMT genotype-phenotype discordant and these were wild-type individuals with low activity (Model III) and heterozygous individuals with normal activity (Model IV). Lists of genes ranked according to the calculated similarity scores for each of the models are presented in the Supplementary tables S2, S3, S4 and S5. For the identification of genes which could be involved in processes causing decreased TPMT activity in individuals with wild-type TPMT genotype, we compared Model I and Model III by calculating differences in individual gene rankings. The analysis showed that genes coding for guanine monophosphate synthase (*GMPS*), aminolevulinic acid dehydratase (*ALAD*), flavin adenine dinucleotide synthetase 1 (*FLAD1*), myotubularin related protein 4 (*MTMR4*), amino adipate-semialdehyde

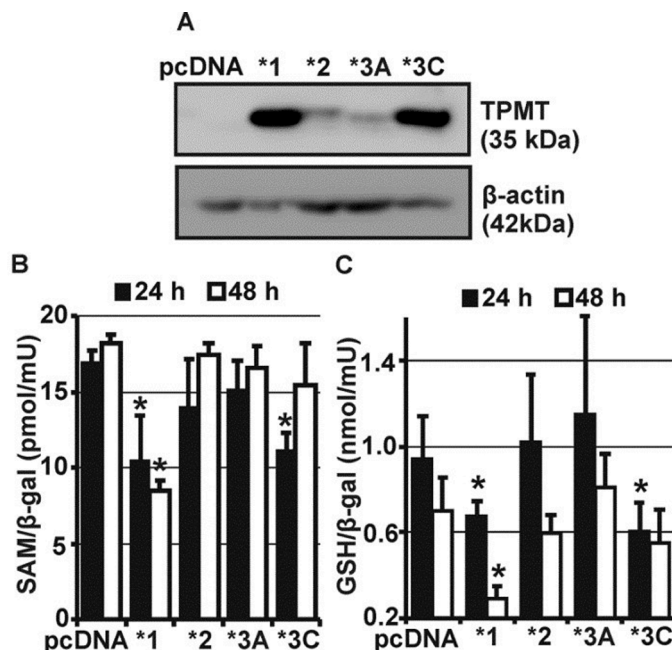


Fig. 6. Differential effects of TPMT allozymes on intracellular SAM and GSH levels.

COS-7 cells were co-transfected with reporter pcDNA3.1/Hygro/lacZ plasmid and pcDNA3.1 vectors containing cDNAs coding for four TPMT allozymes corresponding to the most common genetic polymorphisms (TPMT*1, *2, *3A, *3C). Mock control pcDNA was included in the experiments. (A) TPMT immunoblotting of total cell lysates was carried out to confirm differential levels of recombinant TPMT protein due to non-synonymous amino acid substitutions 24 h post transfection. Intracellular SAM (B) and GSH levels (C) were measured 24 and 48 h post transfection and normalized to cell lysate β-gal activity determined separately (not shown) (**p* < 0.05 vs. pcDNA).

dehydrogenase-phosphopantetheinyl transferase (*AASDHPPT*), and NAD synthetase 1 (*NADSYN1*) were more closely associated with TPMT in the subgroup of individuals with wild-type TPMT genotype and normal enzyme activity (Fig. 7).

On the other hand genes coding for molybdenum cofactor synthesis 2 (*MOCS2*), adenosine deaminase-like (*ADAL*), sulfotransferase family, cytosolic, 1A, phenol-preferring, member 1 (*SULT1A1*), inositol-3-phosphate synthase 1 (*ISYNA1*), guanylate kinase 1 (*GUK1*), phosphoinositide kinase, FYVE finger containing (*PIKFYVE*), aldo-keto reductase family 1, member D1 (*AKR1D1*), and nudix (nucleoside diphosphate linked moiety X)-type motif 10 (*NUDT10*) were more closely associated with TPMT in the subgroup of individuals with wild-type TPMT genotype and low enzyme activity (Fig. 7). When these genes were analysed by AmiGO 2 (Carbon et al., 2009), the statistically significant enrichment of a GO:0019637 term corresponding to organophosphate metabolic process was revealed (Bonferroni corrected *p* value = 3.672e-06), suggesting the involvement of these processes in the regulation of TPMT activity. One of the interesting genes in this group is *MOCS2* coding for molybdenum cofactor synthesis protein 2A and molybdenum cofactor synthesis protein 2B. These two proteins form a molybdopterin synthase complex that catalyzes the conversion of precursor Z into molybdopterin (Reiss et al., 1999). On the other hand, TPMT was recently shown to be involved in catabolism of molybdenum cofactor (Pristup et al., 2022). Furthermore, *MOCS2* is involved in folate biosynthesis pathway, which makes it a plausible candidate gene to further explain fluctuations in TPMT activities, especially since we have previously shown that SAM, the synthesis of which is closely related to folate pathway, influences TPMT activity (Karas-Kuzelićki et al., 2014; Milek et al., 2012). Comparison of Model II (including data from subjects with heterozygous TPMT genotype and low enzyme activity) with Model IV (including data

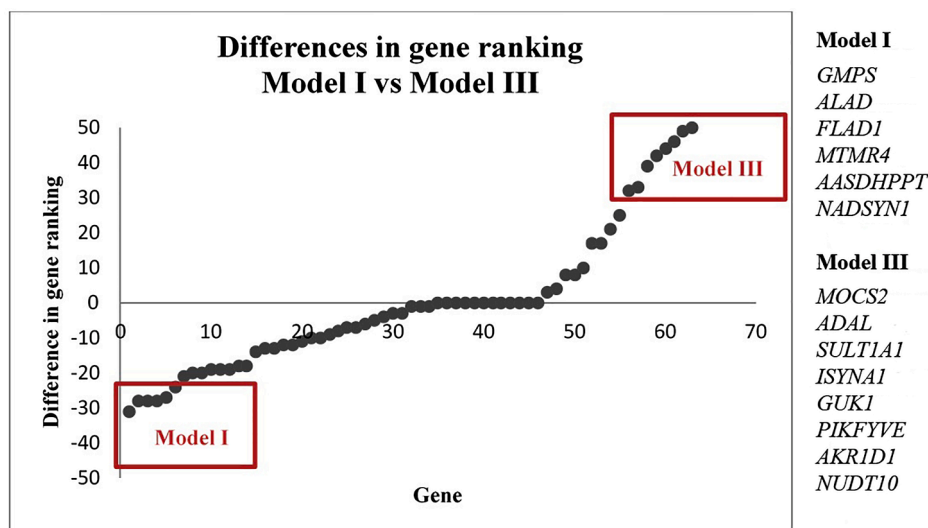


Fig. 7. Comparison of TPMT associated gene rankings between Model I (TPMT wild-type individuals with normal TPMT activity) and Model III (TPMT wild-type individuals with low TPMT activity).

Table on the right lists the genes which are more closely associated with TPMT in each of the groups.

from subjects with heterozygous *TPMT* genotype and normal enzyme activity) did not reveal any significant differences in gene rankings. One of the reasons for this could be in the small number of subjects included to build these two models (46 and 10, respectively). While the current understanding of the precise roles of the identified genes in relation to *TPMT* remains incomplete, a more comprehensive investigation of their functions within *TPMT*-concordant and discordant groups promises to yield valuable insights into endogenous function of *TPMT* and the regulation of its activity. This initiative marks the inception of promising avenues for further molecular research.

4. Conclusions

In the first part of the study on healthy individuals we have used a matrix factorization based data fusion approach (Zitnik and Zupan, 2014). This approach involved the integration of whole genome gene expression data, gene ontology and protein-protein interaction data to explore the *TPMT*-associated gene network and get new insight into its endogenous function.

The constructed model of *TPMT*-associated gene network revealed that *TPMT* is, besides nucleotide and pigment biosynthetic processes, closely related to genes involved in oxidoreductive processes and may thus play an important role in regulating cell redox capacity. In subsequent *in vitro* studies *TPMT* was found to be a pro-oxidative protein due to the facts that it increased toxicity of oxidative stressors and decreased cell antioxidant capacity in HepG2 cells with stable *TPMT* expression and high activity levels. In an *in vitro* model of *TPMT* variants we established that *TPMT* variant proteins, resulting from most common *TPMT* genetic polymorphisms, influence intracellular SAM and GSH status, such that expression of wild-type (*TPMT**1) and *TPMT**3C alleles results in lower methylation and antioxidant capacity, correlating with high *TPMT* activity possibly as a result of less extensive proteasomal degradation. In the event of severe oxidative stress, differential inter-individual phenotypes could emerge in the liver and other tissues due to *TPMT* activity, and further studies should be carried out to test whether more severe hepatotoxicity is observed in wild-type (*TPMT**1) and *TPMT**3C individuals than in individuals with *TPMT**2 and *TPMT**3A polymorphisms.

By comparing models build for subgroups of subjects according to their genotype to phenotype correlation, we identified new candidate genes, among which is also *MOCS2*, which warrant further investigation and could provide new insights into mechanisms of *TPMT* activity

regulation.

CRediT authorship contribution statement

Alenka Šmid: Conceptualization, Formal analysis, Investigation, Visualization, Writing – original draft, Writing – review & editing. **Miha Stajdohar:** Data curation, Formal analysis, Methodology, Writing – review & editing. **Miha Milek:** Investigation, Visualization, Conceptualization, Writing – review & editing. **Dunja Urbančič:** Investigation, Visualization, Writing – review & editing. **Nataša Karas Kuželički:** Conceptualization, Formal analysis, Writing – review & editing. **Riin Tamm:** Investigation, Writing – review & editing. **Andres Metspalu:** Resources, Writing – review & editing. **Irena Mlinarič-Raščan:** Conceptualization, Resources, Writing – review & editing.

Declaration of Competing Interest

The authors have no conflicts of interest that are directly relevant to the content of this article.

Data availability

Data will be made available on request.

Acknowledgments

This work was supported by the Slovenian Research Agency (grant numbers J3-3615, P1-0208) and by the Estonian Gentransmed, Center of Excellence (project nr 2014-2020.4.01. 15-0012).

Supplementary materials

Supplementary material associated with this article can be found, in the online version, at doi:10.1016/j.ejps.2023.106616.

References

- Appell, M.L., Berg, J., Duley, J., Evans, W.E., Kennedy, M.A., Lennard, L., Marinaki, T., McLeod, H.L., Relling, M.V., Schaeffeler, E., Schwab, M., Weinshilboum, R., Yeoh, A. E.J., McDonagh, E.M., Hebert, J.M., Klein, T.E., Coulthard, S.A., 2013. Nomenclature for alleles of the thiopurine methyltransferase gene. *Pharmacogenet. Genom.* 23, 242–248. <https://doi.org/10.1097/FPC.0b013e32835f1cc0>.

- Carbon, S., Ireland, A., Mungall, C.J., Shu, S., Marshall, B., Lewis, S., 2009. AmiGO: online access to ontology and annotation data. *Bioinform. Oxf. Engl.* 25, 288–289. <https://doi.org/10.1093/bioinformatics/btn615>.
- Du, P., Kibbe, W.A., Lin, S.M., 2008. lumi: a pipeline for processing Illumina microarray. *Bioinform. Oxf. Engl.* 24, 1547–1548. <https://doi.org/10.1093/bioinformatics/btn224>.
- Egle, R., Milek, M., Mlinaric-Rascan, I., Fahr, A., Kristl, J., 2008. A novel gene delivery system for stable transfection of thiopurine-S-methyltransferase gene in versatile cell types. *Eur. J. Pharm. Biopharm. Off. J. Arbeitsgemeinschaft Pharm. Verfahrenstechnik EV* 69, 23–30. <https://doi.org/10.1016/j.ejpb.2007.10.004>.
- Estonian Genome Centre, 2023 U.o.T. EGCUT questionnaire.
- Evans, W.E., 2004. Pharmacogenetics of thiopurine S-methyltransferase and thiopurine therapy. *Ther. Drug Monit.* 26, 186–191. <https://doi.org/10.1097/00007691-200404000-00018>.
- Franca, R., Stocco, G., Favretto, D., Giurici, N., del Rizzo, I., Locatelli, F., Vinti, L., Biondi, A., Colombini, A., Fagioli, F., Barisone, E., Pelin, M., Martellosi, S., Ventura, A., Decorti, G., Rabusin, M., 2020. PACSIN2 rs2413739 influence on thiopurine pharmacokinetics: validation studies in pediatric patients. *Pharmacogenom. J.* 20, 415–425. <https://doi.org/10.1038/s41397-019-0130-0>.
- Franco, R., Schoneveld, O., Georgakilas, A.G., Panayiotidis, M.I., 2008. Oxidative stress, DNA methylation and carcinogenesis. *Cancer Lett.* 266, 6–11. <https://doi.org/10.1016/j.canlet.2008.02.026>.
- Fukumoto, Y., Yamada, H., Matsuhashi, K., Okada, W., Tanaka, Y., Suzuki, N., Ogra, Y., 2020. Production of a urinary selenium metabolite, trimethylselenonium, by thiopurine S-methyltransferase and indolethylamine N-methyltransferase. *Chem. Res. Toxicol.* 33, 2467–2474. <https://doi.org/10.1021/acs.chemrestox.0c00254>.
- Geisbrecht, B.V., Gould, S.J., 1999. The human PICD gene encodes a cytoplasmic and peroxisomal NADP(+)-dependent isocitrate dehydrogenase. *J. Biol. Chem.* 274, 30527–30533. <https://doi.org/10.1074/jbc.274.43.30527>.
- Gisbert, J.P., Gomollón, F., Cara, C., Luna, M., González-Lama, Y., Pajares, J.M., Maté, J., Guijarro, L.G., 2007. Thiopurine methyltransferase activity in Spain: a study of 14,545 patients. *Dig. Dis. Sci.* 52, 1262–1269. <https://doi.org/10.1007/s10620-006-9119-z>.
- Hitchler, M.J., Domann, F.E., 2007. An epigenetic perspective on the free radical theory of development. *Free Radic. Biol. Med.* 43, 1023–1036. <https://doi.org/10.1016/j.freeradbiomed.2007.06.027>.
- Hoefs, S.J.G., Skjeldal, O.H., Rodenburg, R.J., Nedregaard, B., van Kaaunen, E.P.M., Spiekerkötter, U., von Kleist-Retzow, J.C., Smeitink, J.A.M., Nijtmans, L.G., van den Heuvel, L.P., 2010. Novel mutations in the NDUFS1 gene cause low residual activities in human complex I deficiencies. *Mol. Genet. Metab.* 100, 251–256. <https://doi.org/10.1016/j.ymgme.2010.03.015>.
- Huang, D.W., Sherman, B.T., Lempicki, R.A., 2009a. Systematic and integrative analysis of large gene lists using DAVID bioinformatics resources. *Nat. Protoc.* 4, 44–57. <https://doi.org/10.1038/nprot.2008.211>.
- Huang, D.W., Sherman, B.T., Lempicki, R.A., 2009b. Bioinformatics enrichment tools: paths toward the comprehensive functional analysis of large gene lists. *Nucleic Acids Res.* 37, 1–13. <https://doi.org/10.1093/nar/gkn923>.
- James, S.J., Melnyk, S., Jernigan, S., Cleves, M.A., Halsted, C.H., Wong, D.H., Cutler, P., Bock, K., Boris, M., Bradstreet, J.J., Baker, S.M., Gaylor, D.W., 2006. Metabolic endophenotype and related genotypes are associated with oxidative stress in children with autism. *Am. J. Med. Genet. Part B Neuropsychiatr. Genet. Off. Publ. Int. Soc. Psychiatr. Genet.* 141B, 947–956. <https://doi.org/10.1002/ajmg.b.30366>.
- Karas Kuzelicki, N., Milek, M., Jazbec, J., Mlinaric-Rascan, I., 2009. 5,10-Methylenetetrahydrofolate reductase (MTHFR) low activity genotypes reduce the risk of relapse-related acute lymphoblastic leukemia (ALL). *Leuk. Res.* 33, 1344–1348. <https://doi.org/10.1016/j.leukres.2008.12.011>.
- Karas-Kuzelicki, N., Šmid, A., Tamm, R., Metspalu, A., Mlinaric-Rascan, I., 2014. From pharmacogenetics to pharmacometabolomics: SAM modulates TPMT activity. *Pharmacogenomics* 15, 1437–1449. <https://doi.org/10.2217/pgs.14.84>.
- Keizer-Garritsen, J.J., Brouwer, C., Lambooy, L.H.J., Ter Riet, P., Bökkerink, J.P.M., Trijbels, F.J.M., De Abreu, R.A., 2003. Measurement of thiopurine S-methyltransferase activity in human blood samples based on high-performance liquid chromatography: reference values in erythrocytes from children. *Ann. Clin. Biochem.* 40, 86–93. <https://doi.org/10.1258/000456303321016222>.
- Kotur, N., Dokmanovic, L., Janic, D., Stankovic, B., Krstovski, N., Tosic, N., Katsila, T., Patrinos, G.P., Zukic, B., Pavlovic, S., 2015. TPMT gene expression is increased during maintenance therapy in childhood acute lymphoblastic leukemia patients in a TPMT gene promoter variable number of tandem repeat-dependent manner. *Pharmacogenomics* 16, 1701–1712. <https://doi.org/10.2217/pgs.15.109>.
- Lennard, L., 1992. The clinical pharmacology of 6-mercaptopurine. *Eur. J. Clin. Pharmacol.* 43, 329–339. <https://doi.org/10.1007/BF02220605>.
- Lennard, L., Cartwright, C.S., Wade, R., Richards, S.M., Vora, A., 2013. Thiopurine methyltransferase genotype-phenotype discordance and thiopurine active metabolite formation in childhood acute lymphoblastic leukaemia. *Br. J. Clin. Pharmacol.* 76, 125–136. <https://doi.org/10.1111/bcp.12066>.
- Lin, C.L., Huang, H.C., Lin, J.K., 2007. Theaflavins attenuate hepatic lipid accumulation through activating AMPK in human HepG2 cells. *J. Lipid Res.* 48, 2334–2343. <https://doi.org/10.1194/jlr.M700128-JLR200>.
- McLeod, H.L., Krynetski, E.Y., Wilimas, J.A., Evans, W.E., 1995. Higher activity of polymorphic thiopurine S-methyltransferase in erythrocytes from neonates compared to adults. *Pharmacogenetics* 5, 281–286. <https://doi.org/10.1097/00008571-199510000-00003>.
- Milek, M., Karas Kuzelicki, N., Šmid, A., Mlinaric-Rascan, I., 2009. S-adenosylmethionine regulates thiopurine methyltransferase activity and decreases 6-mercaptopurine cytotoxicity in MOLT lymphoblasts. *Biochem. Pharmacol.* 77, 1845–1853. <https://doi.org/10.1016/j.bcp.2009.03.006>.
- Milek, M., Murn, J., Jaksic, Z., Lukac Bajalo, J., Jazbec, J., Mlinaric Rascan, I., 2006. Thiopurine S-methyltransferase pharmacogenetics: genotype to phenotype correlation in the Slovenian population. *Pharmacology* 77, 105–114. <https://doi.org/10.1159/000093278>.
- Milek, M., Šmid, A., Tamm, R., Kuzelicki, N.K., Metspalu, A., Mlinaric-Rascan, I., 2012. Post-translational stabilization of thiopurine S-methyltransferase by S-adenosyl-L-methionine reveals regulation of TPMT*1 and *3C allozymes. *Biochem. Pharmacol.* 83, 969–976. <https://doi.org/10.1016/j.bcp.2012.01.010>.
- Miller, S.A., Dykes, D.D., Polesky, H.F., 1988. A simple salting out procedure for extracting DNA from human nucleated cells. *Nucleic Acids Res.* 16, 1215. <https://doi.org/10.1093/nar/16.3.1215>.
- Mosharov, E., Cranford, M.R., Banerjee, R., 2000. The quantitatively important relationship between homocysteine metabolism and glutathione synthesis by the transsulfuration pathway and its regulation by redox changes. *Biochemistry* 39, 13005–13011. <https://doi.org/10.1021/bi001088w>.
- Pristup, J., Schaeffeler, E., Arjune, S., Hofmann, U., Angel Santamaria-Araujo, J., Leuthold, P., Friedrich, N., Nauck, M., Mayr, S., Haag, M., Muerdter, T., Marner, F.J., Relling, M.V., Evans, W.E., Schwarz, G., Schwab, M., 2022. Molybdenum cofactor catabolism unravels the physiological role of the drug metabolizing enzyme thiopurine S-methyltransferase. *Clin. Pharmacol. Ther.* 112, 808–816. <https://doi.org/10.1002/cpt.2637>.
- Reiss, J., Dorche, C., Stallmeyer, B., Mendel, R.R., Cohen, N., Zabet, M.T., 1999. Human molybdopterine synthase gene: genomic structure and mutations in molybdenum cofactor deficiency type B. *Am. J. Hum. Genet.* 64, 706–711. <https://doi.org/10.1086/302296>.
- Relling, M.V., Gardner, E.E., Sandborn, W.J., Schmiegelow, K., Pui, C.H., Yee, S.W., Stein, C.M., Carrillo, M., Evans, W.E., Klein, T.E., Clinical Pharmacogenetics Implementation Consortium, 2011. Clinical pharmacogenetics implementation consortium guidelines for thiopurine methyltransferase genotype and thiopurine dosing. *Clin. Pharmacol. Ther.* 89, 387–391. <https://doi.org/10.1038/clpt.2010.320>.
- Santos, C.X.C., Anilkumar, N., Zhang, M., Brewer, A.C., Shah, A.M., 2011. Redox signaling in cardiac myocytes. *Free Radic. Biol. Med.* 50, 777–793. <https://doi.org/10.1016/j.freeradbiomed.2011.01.003>.
- Schaeffeler, E., Fischer, C., Brockmeier, D., Wernet, D., Moerike, K., Eichelbaum, M., Zanger, U.M., Schwab, M., 2004. Comprehensive analysis of thiopurine S-methyltransferase phenotype-genotype correlation in a large population of German-Caucasians and identification of novel TPMT variants. *Pharmacogenetics* 14, 407–417. <https://doi.org/10.1097/01.fpc.0000114745.08559.db>.
- Serpe, L., Calvo, P.L., Muntoni, E., D'Antico, S., Giaccone, M., Avagnina, A., Baldi, M., Barbera, C., Curti, F., Pera, A., Eandi, M., Zara, G.P., Canaparo, R., 2009. Thiopurine S-methyltransferase pharmacogenetics in a large-scale healthy Italian-Caucasian population: differences in enzyme activity. *Pharmacogenomics* 10, 1753–1765. <https://doi.org/10.2217/pgs.09.103>.
- Šmid, A., Karas-Kuzelicki, N., Jazbec, J., Mlinaric-Rascan, I., 2016. PACSIN2 polymorphism is associated with thiopurine-induced hematological toxicity in children with acute lymphoblastic leukaemia undergoing maintenance therapy. *Sci. Rep.* 6, 30244. <https://doi.org/10.1038/srep30244>.
- Spire-Vayron de la Moureyre, C., Debusere, H., Mastain, B., Vinner, E., Marez, D., Lo Guidice, J.M., Chevalier, D., Brique, S., Motte, K., Colombel, J.F., Turck, D., Noel, C., Flipo, R.M., Pol, A., Lhermitte, M., Lafitte, J.J., Libersa, C., Broly, F., 1998. Genotypic and phenotypic analysis of the polymorphic thiopurine S-methyltransferase gene (TPMT) in a European population. *Br. J. Pharmacol.* 125, 879–887. <https://doi.org/10.1038/sj.bjp.0702152>.
- Stocco, G., Yang, W., Crews, K.R., Thierfelder, W.E., Decorti, G., Londero, M., Franca, R., Rabusin, M., Valsecchi, M.G., Pei, D., Cheng, C., Pough, S.W., Ramsey, L.B., Diouf, B., McCorkle, J.R., Jones, T.S., Pui, C.H., Relling, M.V., Evans, W.E., 2012. PACSIN2 polymorphism influences TPMT activity and mercaptopurine-related gastrointestinal toxicity. *Hum. Mol. Genet.* 21, 4793–4804. <https://doi.org/10.1093/hmg/dds302>.
- Tai, H.L., Krynetski, E.Y., Schuetz, E.G., Yanishevski, Y., Evans, W.E., 1997. Enhanced proteolysis of thiopurine S-methyltransferase (TPMT) encoded by mutant alleles in humans (TPMT*3A, TPMT*2): mechanisms for the genetic polymorphism of TPMT activity. *Proc. Natl. Acad. Sci. U. S. A.* 94, 6444–6449. <https://doi.org/10.1073/pnas.94.12.6444>.
- Urbančić, D., Kotar, A., Šmid, A., Jukić, M., Gobec, S., Mårtensson, L.G., Plavec, J., Mlinaric-Rascan, I., 2019. Methylation of selenocysteine catalysed by thiopurine S-methyltransferase. *Biochim. Biophys. Acta Gen. Subj.* 1863, 182–190. <https://doi.org/10.1016/j.bbagen.2018.10.002>.
- Urbančić, D., Šmid, A., Stocco, G., Decorti, G., Mlinaric-Rascan, I., Karas Kuzelicki, N., 2018. Novel motif of variable number of tandem repeats in TPMT promoter region and evolutionary association of variable number of tandem repeats with TPMT*3 alleles. *Pharmacogenomics* 19, 1311–1322. <https://doi.org/10.2217/pgs-2018-0123>.
- Wang, W., Kramer, P.M., Yang, S., Pereira, M.A., Tao, L., 2001. Reversed-phase high-performance liquid chromatography procedure for the simultaneous determination of S-adenosyl-L-methionine and S-adenosyl-L-homocysteine in mouse liver and the effect of methionine on their concentrations. *J. Chromatogr. B. Biomed. Sci. App.* 762, 59–65. [https://doi.org/10.1016/S0378-4347\(01\)00341-3](https://doi.org/10.1016/S0378-4347(01)00341-3).
- Weinshilboum, R.M., Sladek, S.L., 1980. Mercaptopurine pharmacogenetics: monogenic inheritance of erythrocyte thiopurine methyltransferase activity. *Am. J. Hum. Genet.* 32, 651–662.
- Wennerstrand, P., Mårtensson, L.G., Söderhäll, S., Zimdahl, A., Appell, M.L., 2013. Methotrexate binds to recombinant thiopurine S-methyltransferase and inhibits enzyme activity after high-dose infusions in childhood leukaemia. *Eur. J. Clin. Pharmacol.* 69, 1641–1649. <https://doi.org/10.1007/s00228-013-1521-9>.

- Yates, C.R., Krynetski, E.Y., Loennechen, T., Fessing, M.Y., Tai, H.L., Pui, C.H., Relling, M.V., Evans, W.E., 1997. Molecular diagnosis of thiopurine S-methyltransferase deficiency: genetic basis for azathioprine and mercaptopurine intolerance. *Ann. Internal Med.* 126, 608–614. <https://doi.org/10.7326/0003-4819-126-8-199704150-00003>.
- Zimdahl Kahlin, A., Helander, S., Wennerstrand, P., Vikingsson, S., Mårtensson, L., Appell, M.L., 2021. Pharmacogenetic studies of thiopurine methyltransferase genotype-phenotype concordance and effect of methotrexate on thiopurine metabolism. *Basic Clin. Pharmacol. Toxicol.* 128, 52–65. <https://doi.org/10.1111/bcpt.13483>.
- Zitnik, M., Zupan, B., 2014. Matrix factorization-based data fusion for gene function prediction in baker's yeast and slime mold. *Pac. Symp. Biocomput. Pac. Symp. Biocomput.* 400–411.
- Zudeh, G., Franca, R., Lucafò, M., Bonten, E.J., Bramuzzo, M., Sgarra, R., Lagatolla, C., Franzin, M., Evans, W.E., Decorti, G., Stocco, G., 2023. PACSIN2 as a modulator of autophagy and mercaptopurine cytotoxicity: mechanisms in lymphoid and intestinal cells. *Life Sci. Alliance* 6. <https://doi.org/10.26508/lsa.202201610>.